

A Single Image Super Resolution Using Advanced Neighbor Embedding

Dr. S. D. Ruikar

Department of E&TC,
Sinhgad Academy of Engineering,
Pune, India
ruikaretcdept@gmail.com

Mr. T.D. Wadhavane

Department of E&TC,
Sinhgad Academy of Engineering,
Pune, India
tush.org@gmail.com

Abstract— There are lots of Super resolution methods developed recently. Each has its own pros and cons and behavior. The neighbor-embedding (NE) algorithm for single-image super-resolution reconstruction is one of them which assume that the feature spaces of low-resolution and high-resolution patches are locally isometric. Even, this is not true for SR because of one to many mappings between Low Resolution and High Resolution patches. To minimize the problem for NE-based SR reconstruction, an advanced Neighbor Embedding based method for Super resolution used in which combine learning technique used to train two projection matrices simultaneously and to map the original Low Resolution and High Resolution feature spaces onto a unified feature subspace. Reconstruction weights of the k-Nearest neighbour of Low Resolution image patches is found by performing operation on those Low Resolution patches in unified feature space. To handle a large number of samples, combine learning use a coupled constraint by linking the LR–HR counterparts together with the k-nearest grouping patch pairs. The Advanced NE algorithm gives better resolution and outperforms NE method for image super resolution.

Keywords- Grouping patch pairs (GPPs), combine learning, neighbor embedding (NE), super-resolution (SR).

I. INTRODUCTION

A Digital imaging system has lot of limitations, the imaging environment also important part of capturing an image, so it is not always easy to capture an image at a desired high-resolution (HR) level. However, in many practical applications such as medical imaging, video surveillance, computer vision, and entertainment, HR images are required usually to obtain a robust performance. Therefore, it becomes popular to synthesize a new HR image by using one or more low-resolution (LR) images [1].

The fast interpolation methods such as bilinear, bi-cubic, and other resampling methods [2]–[3] can increase the size of LR input, they are prone to blur high-frequency details and not super resolve the LR image, they only up-sample the image. Thus, a large number of super-resolution (SR) reconstruction techniques have been developed in recent years, which can be divided into two categories: multi image-based SR methods and example learning-based SR methods [4], [5].

There are two types of multi-image-based SR methods: The frequency-domain methods [6]–[7] and spatial-domain methods [8]–[9]. It has been proved that the spatial representation of super resolution gives better performance than the frequency domain one. Representative spatial-domain methods include the regularized SR reconstruction approaches [10]–[11], the projection-onto-convex-sets approach [12], iterative back projection (IBP) [13], adaptive filtering [14], nonlocal means [15]–[16], and nonlocal kernel regression [9]. But all the above mention methods require adequate number of LR images. Example learning based group of SR methods assumes that the high-frequency details lost in an LR image can be learned from a training set of LR and HR image pairs, i.e., the relationship between LR image patches and the corresponding HR patches can be used to estimate the missing HR frequency details in the given LR input. The example learning based method assumed that the counterparts of LR–HR image patch pairs (or their feature representations) are locally isometric. In contrast to above methods, this neighbor-embedding (NE)-based method does not require a large number of samples and achieves top level performance.

When the magnification increase (e.g., more than *3 up-scaling), the SR problem becomes severely undetermined. Thus, the correspondence between the LR image patches and the HR image patches in NE-based methods becomes ambiguous, i.e., the neighborhood relationship cannot be preserved perfectly due to the “one-to-many” mapping existing between one LR image and many HR images. For NE-based methods, a crucial

problem is preserving the neighbourhood relationship of each LR and its HR counterpart as consistently as possible. In addition, an inappropriate number of neighbors may end up with under fitting or over fitting of the result. Note that the choice of the neighborhood size affects linear embedding of edge patches and of non-edge patches.

II. ADVANCE NEIGHBOR EMBEDDING BASED SUPER RESOLUTION

In this section, a MAP reconstruction framework for SR is discussed. A coupled constraint on k -NNs of LR–HR counterparts, i.e., GPPs (grouping patch pairs), is then established for the combine learning process. Thereafter, for each LR image patch to be super-resolved, its nearest GPPs (including k -NNs of LR–HR image patch pairs) is searched to perform combine learning for the unified feature subspace. Subsequently, the selection of k -NNs and the optimal weights for reconstruction are performed in the unified feature subspace for the initial HR output patches. Fig. 1 illustrates the reconstruction framework of Advance NE algorithm.

- The coupled constraint on GPPs consisting of the LR–HR image patches is applied to the learning process, which ensures a better consistency local LR and HR image patches.
- Matrices P_l and P_h are the mapping matrices obtain from combine learning such that the difference between LR–HR counterparts is reduced as much as possible in the unified feature subspace. The optimal reconstruction weights for SR reconstruction are then estimated in the unified feature subspace rather than solely in the LR feature space.

A. MAP Reconstruction Framework

HR images can be divided into three sub-bands, the high frequency band I_h , the middle frequency band I_m and the low frequency band I_l . The middle-frequency components can be recovered based upon a simple interpolation algorithm (e.g., bilinear or bicubic). Thus, the goal of SR reconstruction is to estimate the missing high-frequency component with a single LR input. If prior knowledge, which is denoted as manifold MF, can be incorporated into the SR process, the problem of SR reconstruction can be written as,

$$I_h^* = \arg \max_{I_h} P(I_h | I_l, MF) \quad (1)$$

By using Beyes rule, (1) becomes,

$$I_h^* = \arg \max_{I_h} P(MF | I_h, I_l) P(I_l | I_h) P(I_h) \quad (2)$$

Taking the negative log likelihood $E = -\log(p(\cdot))$ in (2), we can get,

$$I_h^* = \arg \min_{I_h} E(MF | I_h, I_l) + E(I_l | I_h) + E(I_h) \quad (3)$$

Where f_l and f_h denote two mapping functions used to convert two different feature vectors x_s^i and y_s^i into a unified feature space. In this way, use a common distance metric to measure the similarity between them.

The term $E(I_l | I_h)$ stands for the data cost of the reconstruction error of all input LR image patches with respect to their neighbourhood $N_g(\cdot)$ i.e.

$$E(I_l | I_h) = \sum_j \left\| f_l(x_l^j) - \sum_{i \in N_g(j)} w_{ij} f_h(y_h^i) \right\|_2^2 \quad (4)$$

The term $E(I_h)$ can be seen as the smoothness prior of the HR image, which can be approximated by overlapping one or several pixels within the adjacent image patches. Therefore, the key problem to solve is finding the two mapping functions f_l and f_h to transform the LR and HR feature spaces into a unified feature subspace. Once achieved, utilize the traditional NE algorithm to estimate the optimal weights and generate the desired HR image patch as a linear combination of the corresponding HR image patches from its neighbors. In addition, the problem of finding M_j associated with each x_s^i remains unresolved. This problem is addressed by grouping the k -nearest group patch pairs of the LR and HR features in the training data set.

B. Coupled Constraint

In NE method [17], the training data set of the LR image patches, $X_s = [x_s^i]_{i=1}^N$ and that of their corresponding HR image patches $Y_s = [y_s^i]_{i=1}^N$ where represents the index of each image patch and N is the

number of image patches collected. In the traditional NE for SR x_s^i represents a d -dimensional feature vector of the i th LR image patch by concatenating the first- and second-order gradient features in horizontal and vertical directions, respectively. The y_s^i is the high frequency details of the i -th HR image patch. In order to apply combine learning to two different feature spaces of LR and HR patches, and augment another training data set $Z_s = [z_s^i]_{i=1}^N$ that consists of the first- and second-order gradient features of HR image patches in horizontal and vertical directions, which is similar to the representation of each LR image patch. In such way z_s^i , denotes an m -dimensional feature vector of the i th HR image patch.

Most existing NE algorithms perform SR reconstruction without considering the correlation between the LR and HR image patches. That means that they solely apply an isometric assumption to synthesize the expected HR estimates. However, this assumption does not hold perfectly for the SR problem. To solve or at least to reduce this problem, Advance NE considers the similarity between the LR image patch and the HR image patch with a coupled constraint as follows.

Let $C = [c^i]_{i=1}^N$ be a coupled set by concatenating each feature vector x_s^i and y_s^i . Thus, each column measurement c^i in set C is a $(d+m)$ dimensional feature vector, i.e.

$$c_i = \begin{bmatrix} x_s^i / \sqrt{d} \\ y_s^i / \sqrt{m} \end{bmatrix} \quad (5)$$

To adjust the dynamic changes of the concatenated feature Vector, normalize it to a unit two-norm. For each vector C^i in Set C , select the k -NNs associated with it and group them Together by

$$G^i \overset{\Delta}{=} \{C_J\}_{J \in N_k(i)} \quad (6)$$

Where $G^i (1 \leq i \leq N)$ stands for the i -th GPPs related to x_s^i and $N_k(i)$ represents the index set of k -NNs of C_i

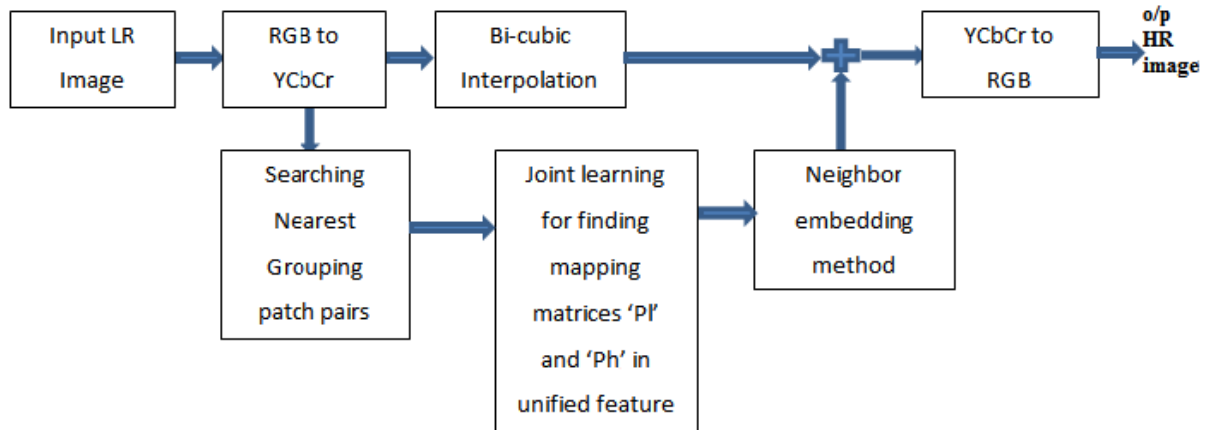


Fig.1. Advance NE method reconstruction

C. Combine Learning on Patch Pairs

Under the MAP reconstruction framework described in Section II-A, find the two mapping functions f_l and f_h to project the LR and HR feature spaces onto a unified feature subspace. Then apply combine learning to transform two feature spaces spanned by different dimensional feature vectors into a unified feature subspace.

Let $L^i = R^{d*k} (i = 1, \dots, N)$ denote the constraint patch matrix by stacking K d -dimensional column vectors whose indices are specified in G_i , i.e. $L^i = \{x_s^r\}_{r \in G^i}$. Similarly, $H^i = R^{m*k} (i = 1, \dots, N)$ and $H^i = \{z_s^r\}_{r \in G^i}$. The existing NE-based SR [17] measures the similarity in the LR feature space. Generally,

these algorithms make an assumption that the relationship between LR and HR feature spaces is locally isometric, i.e., the neighbor relationship between the LR and HR feature spaces is locally preserved.

LR and HR features can share a unified feature subspace in which they are more closely associated with each other as in [18]. Based on this consideration, the feature representations of LR and HR counterparts are projected onto a unified feature subspace by combine learning via a coupled constraint. Following this, the selection of k-NNs is conducted in this unified feature subspace instead of the original LR space. The combine learning on the GPP of each LR input locally also performed, rather than on all training samples, which is efficient and tractable for a training data set containing an enormous number of samples.

In unified feature space two mapping matrices are measured one is for the LR feature space

$f_l = R^D \rightarrow R^P$ and another is for HR feature space $f_h = R^m \rightarrow R^P$. In this way, project the LR and HR feature spaces simultaneously onto a unified feature subspace and measure their similarity by

$$d_{ij} = Dist(f_l(x_s^i), f_h(z_s^i)) \tag{7}$$

Whereas function distance (Dist(.)) represent Euclidean distance.

For (7), the problem is converted to construct the mapping functions f_l and f_h such that distance d_{ij} should be as close as possible in the unified feature subspace. If the similarity is measured by the Euclidean distance, then

$$\arg \min_{\{f_l, f_h\}} \sum_{i \in G^i} \|f_l(x_s^i) - f_h(z_s^i)\|_2^2 \tag{8}$$

Suppose the two mapping functions f_l and f_h are represented by projection matrices

$P_l \in R^{d \times p}$ and $P_h \in R^{m \times p}$ then eq. (8) can modify as-

$$\arg \min_{\{P_l, P_h\}} \sum_{i \in G^i} \|P_l^T x_s^i - P_h^T z_s^i\|_2^2 \tag{9}$$

$$\arg \min_{\{P_l, P_h\}} tr \left(\begin{bmatrix} P_l \\ P_h \end{bmatrix}^T \begin{bmatrix} L^i & 0 \\ 0 & H^i \end{bmatrix} \begin{bmatrix} I & -I \\ -I & I \end{bmatrix} \times \begin{bmatrix} L^i & 0 \\ 0 & H^i \end{bmatrix} \begin{bmatrix} P_l \\ P_h \end{bmatrix} \right) \tag{10}$$

$$\arg \min_P tr(P^T S A S^T P) \tag{11}$$

This equation (11) obtain by assigning P, S, A to matrices shown in eq. (10) respectively.

Suppose that $E = S A S^T$ and $F = S S^T$, the optimization problem with respect to P can be obtained by the eigenvectors p of $E_p = \lambda F_p$ associated with the second to the p-th ($P \leq d$) smallest eigenvalues. Here, matrices E and F are of size $(d + m) \times (d + m)$. For the solutions to p_l and p_h , expand the $E_p = \lambda F_p$ to two linear equations, i.e.,

$$L^i (L^i)^T p_l - L^i (H^i)^T p_h = \lambda L^i (L^i)^T p_l \tag{12}$$

$$H^i (H^i)^T p_h - H^i (L^i)^T p_l = \lambda H^i (H^i)^T p_h \tag{13}$$

From (13), the solution to p_h can be obtained from,

$$P_h = \frac{(H^i (H^i)^T)^{-1} H^i (L^i)^T P_l}{(1 - \lambda)} \tag{14}$$

According to (14), eliminate p_h in (12) and obtain

$$H^i (H^i)^T (H^i (H^i)^T)^{-1} H^i (L^i)^T p_l = (1 - \lambda)^2 L^i (L^i)^T p_l \tag{15}$$

Let eq. (15) reduces to (16) by replacing, U and V.

$$U_{pl} = (1 - \lambda)^2 V_{pl} \tag{16}$$

Once P_l is obtained, substitute it into (13) for P_h . By selecting the appropriate dimension of the p subspace (or the unified feature subspace), use the two derived projection matrices P_l and P_h to transform the original LR and HR feature spaces into a common subspace. In this way, the selection of k-NNs can be conducted within the unified feature subspace. Combine learning for the projection matrices is summarized in algorithm.

Algorithm 1 (Combine Learning for Projection Matrices)

Input parameters:

- Training data set $X_s = \{x_s^i\}_{i=1}^N$ and $Z_s = \{z_s^i\}_{i=1}^N$
- GPPs set $\{G^i\}_{i=1}^N$;
- LR patch x_t^j in the test data set X_t

Output parameters:

- Projection matrices P_l and P_h ;
- Constraint patches matrices L^i and H^i .

Description:

1. Find the nearest neighbour x_s^i related to x_t^j in the training data set X_s .
2. Obtain the GPPs G^i corresponding to x_s^i .
3. According to the index se specified in G^i , build the constraint patch matrices L^i and H^i respectively.
4. Construct projection matrices P_l and P_h .

Algorithm 2 (Advance Neighbor Embedding)

Input parameters:

- Training data set $X_s = \{x_s^i\}_{i=1}^N$, $Y_s = \{y_s^i\}_{i=1}^N$ and $Z_s = \{z_s^i\}_{i=1}^N$
- GPPs set $\{G^i\}_{i=1}^N$; LR image ;
- The size of LR image patch $q \times q$;
- Neighborhood size k ;
- Dimension P of the unified feature subspace to be projected.

Output parameters:

- HR image Y

Description:

1. Partition Y into $q \times q$ image patches with one or two pixels overlapped in raster-scan order to construct the test data set $X_t = \{x_t^i\}_{i=1}^M$
2. For each patch x_t^j in X_t , execute the following steps repeatedly:
 - Compute the mean values \bar{x} of patch x_t^j
 - Construct the constraint patch matrices P_l and P_h related to the nearest neighbour x_s^i of x_t^j and compute the projection matrices P_l and P_h associated with x_t^j with algorithm 1.
 - Compute the transformed feature of x_t^j via $P_l^T x_t^j$ and project the coupled constraint patches L^i and H^i the unified feature subspace via $P_l^T L^i$ and $P_h^T H^i$ respectively.
 - Compute the optimal weights by minimizing reconstruction error as follows:

$$\arg \min_{\{w_{i,j}\}} \left\| P_l^T x_t^j - \sum_{i \in N_g(j)} w_{ij} P_h^T H^i \right\|_2^2 \quad (17)$$

- Reconstruct each y_t^j corresponding to x_t^j with the optimal weights w_{ij} as follows:

$$y_t^j = \sum_{i \in N_g(j)} w_{ij} y_s^i \quad (18)$$

- Sum up mean values \bar{x} and y_t^j together to generate the HR patch y_t^j and append it to Y_t .
3. Produce the initial HR image X_0 by merging all the HR patches in the set $Y_t = \{y_t^j\}_{j=1}^M$ for the overlapping region between those adjacent patches, averaging fusion is applied to obtain the estimated pixels.

III. EXPERIMENTAL RESULTS

The PSNR obtained for the different images is given in table below. And the SR results of different images shown in fig. 2, 3, and 4 respectively.

	Nearest Neighbour Interpolation	Bilinear Interpolation	Bicubic Interpolation	Advance NE
X-Ray Image	30.7624	32.3488	32.9778	33.4203
Flower Image	27.7198	29.5637	30.5051	30.6765
Bird Image	25.0546	26.1977	26.8135	27.3939

TABLE 1. PSNR

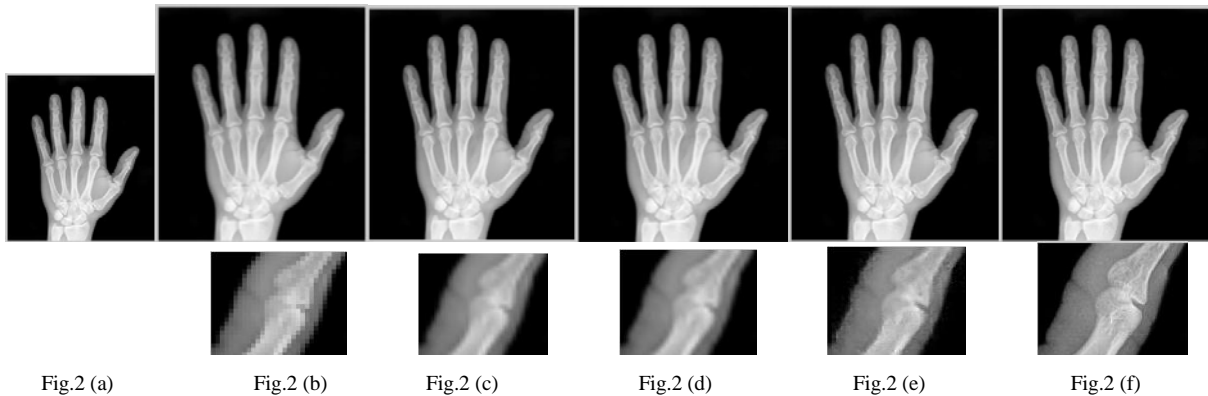


Fig. 2 shows results for X-Ray image. (The image under main image is particular part after zooming)

Fig.2 (a) is down-sampled version of original image. Fig.2 (b) is High-Resolution image obtained from Nearest Neighbor Interpolation method. Fig.2 (c) is High-Resolution image obtained from Bilinear Interpolation method. Fig.2 (d) is High-Resolution image obtained from Bicubic Interpolation method and Fig.2 (e) is High-Resolution image obtained from Advance NE method and Fig.2 (f) is the original High-resolution image.

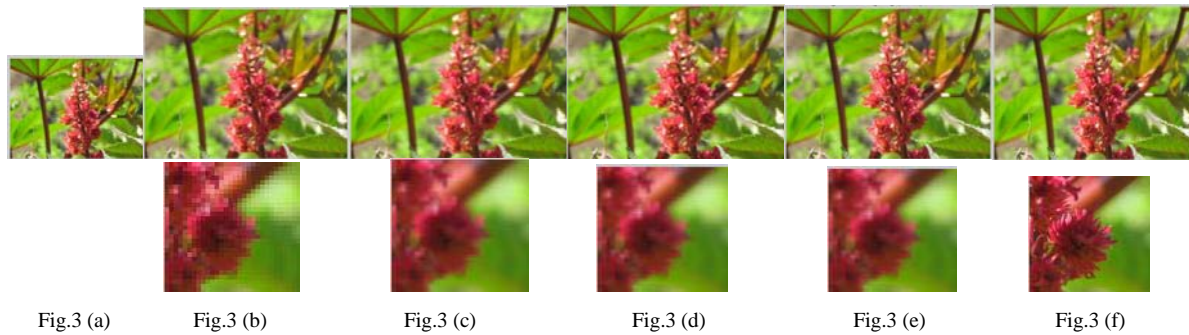


Fig. 3 shows results for Flower image. . (The image under main image is particular part after zooming)

Fig.3 (a) is down-sampled version of original image. Fig.3 (b) is High-Resolution image obtained from Nearest Neighbor Interpolation method. Fig.3 (c) is High-Resolution image obtained from Bilinear Interpolation method. Fig.3 (d) is High-Resolution image obtained from Bi-cubic Interpolation method and Fig.3 (e) is High-Resolution image obtained from Advance NE method and Fig.3 (f) is the original High-resolution image.

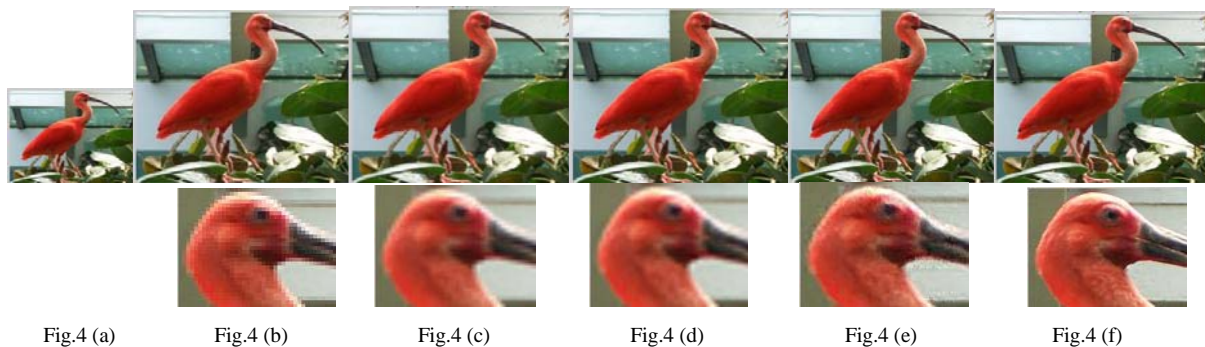


Fig. 4 shows results for Bird image.

Fig.4 (a) is down-sampled version of original image. Fig.4 (b) is High-Resolution image obtained from Nearest Neighbor Interpolation method. Fig.4 (c) is High-Resolution image obtained from Bilinear Interpolation method. Fig.4 (d) is High Resolution image obtained from Bi-cubic Interpolation method and Fig.4 (e) is High-Resolution image obtained from Advance NE method and Fig.4 (f) is the original High resolution image.

IV. CONCLUSION

This paper has introduced Advance Neighbor Embedding based single-image SR reconstruction. The experimental result shows that Advance NE method gives the best SR output. The most important part in advance NE is the selection of k -NNs and the linear embedding being performed in the unified feature subspace rather than in the original LR space. In order to obtain the formation process of the LR image from its HR version, all the training HR images are down-sampled by using the bi-cubic interpolation by a factor of 3 to obtain the corresponding LR images. Since the human visual system (HVS) is more sensitive to the luminance component than the chrominance components, Use of the YCbCr color space for color images and only perform SR reconstruction in the luminance component. Considering that the middle-frequency information of LR images has greater correlation with high frequency than low frequency, first magnify the original LR input by a factor of 2 with the bi-cubic interpolation and then perform SR on it. In this implementation, the combine learning technique on GPPs those are most relevant to each LR input patch to obtain the desired unified feature subspace. In principle, the Advance NE method has the potential to be extended to other SR applications such as face image hallucination. In addition, the construction of optimal GPPs rather than a fixed neighborhood size is challenging for this method.

V. REFERENCES

- [1] S. Park, M. Park, and M. Kang, "Super-resolution image reconstruction: A technical overview," *IEEE Signal Process. Mag.*, vol. 20, no. 3, pp. 21–36, May 2003.
- [2] X. Li and M. T. Orchard, "New edge-directed interpolation," *IEEE Trans. Image Process.*, vol. 10, no. 10, pp. 1521–1527, Oct. 2001.
- [3] K. S. Ni and T. Q. Nguyen, "An adaptable k -nearest neighbors algorithm for MMSE image interpolation," *IEEE Trans. Image Process.*, vol. 18, no. 9, pp. 1976–1987, Sep. 2009.
- [4] D. Glasner, S. Bagon, and M. Irani, "Super-resolution from a single image," in Proc. IEEE Int. Conf. Comput. Vis., 2009, pp. 349–356.
- [5] J. Sun, Q. Chen, S. Yan, and L.-F. Cheong, "Selective image super-resolution," Computer Vision and Pattern Recognition 2010, arXiv: 1010.5610v1.
- [6] T. S. Huang and R. Y. Tsai, "Multi-frame image restoration and registration," *Adv. Comput. Vis. Image Process.*, vol. 1, no. 2, pp. 317–339, 1984.

- [7] S. P. Kim and W. Y. Su, "Recursive high-resolution reconstruction of blurred multiframe images," *IEEE Trans. Image Process.*, vol. 2, no. 4, pp. 534–539, Oct. 1993.
- [8] S. P. Kim, N. K. Bose, and H. M. Valenzuela, "Recursive reconstruction of high resolution image from noisy undersampled multiframes," *IEEE Trans. Acoust., Speech, Signal Process.*, vol. 38, no. 6, pp. 1013–1027, Jun. 1990.
- [9] H. Zhang, J. Yang, Y. Zhang, and T. S. Huang, "Non-local kernel regression for image and video restoration," in *Proc. Eur. Conf. Comput. Vis.*, 2010, pp. 566–579.
- [10] M. C. Hong, M. G. Kang, and A. K. Katsaggelos, "A regularized multichannel restoration approach for globally optimal high resolution video sequence," in *Proc. SPIE VCIP*, San Jose, CA, Feb. 1997, vol. 3024, pp. 1306–1317.
- [11] X. Li, X. Gao, Y. Hu, D. Tao, and B. Ning, "A multi-frame image super-resolution method," *Signal Process.*, vol. 90, no. 2, pp. 405–414, Feb. 2010.
- [12] H. Stark and P. Oskoui, "High-resolution image recovery from image plane arrays, using convex projections," *J. Opt. Soc. Amer. A, Opt. Image Sci., Vis.*, vol. 6, no. 11, pp. 1715–1726, Nov. 1989.
- [13] M. Irani and S. Peleg, "Improving resolution by image registration," *CVGIP, Graph. Models Image Process.*, vol. 53, no. 3, pp. 231–239, May 1991.
- [14] M. Elad and A. Feuer, "Superresolution restoration of an image sequence: Adaptive filtering approach," *IEEE Trans. Image Process.*, vol. 8, no. 3, pp. 387–395, Mar. 1999.
- [15] M. Protter and M. Elad, "Super resolution with probabilistic motion estimation," *IEEE Trans. Image Process.*, vol. 18, no. 8, pp. 1899–1904, Aug. 2009.
- [16] X. Gao, Q. Wang, X. Li, D. Tao, and K. Zhang, "Zernike-momentbased image super resolution," *IEEE Trans. Image Process.*, vol. 20, no. 10, Oct. 2011.
- [17] H. Chang, D.-Y. Yeung, and Y. Xiong, "Super-resolution through neighbor embedding," in *Proc. IEEE Conf. Comput. Vis. Pattern Recog.*, Jul. 2004, pp. 275–282.
- [18] B. Li, H. Chang, S. Shan, and X. Chen, "Low-resolution face recognition via coupled local preserving mappings," *IEEE Signal Process. Lett.*, vol. 17, no. 1, pp. 20–23, Jan. 2010.
- [19] L. Zhang and X. Wu, "An edge-guided image interpolation algorithm via directional filtering and data fusion," *IEEE Trans. Image Process.*, vol. 15, no. 8, pp. 2226–2238, Aug. 2006.
- [20] S. Farsiu, M. D. Robinson, M. Elad, and P. Milanfar, "Fast and robust multi-frame super resolution," *IEEE Trans. Image Process.*, vol. 13, no. 10, pp. 1327–1344, Oct. 2004.
- [21] H. Takeda, P. Milanfar, M. Protter, and M. Elad, "Super-resolution without explicit subpixel motion estimation," *IEEE Trans. Image Process.*, vol. 18, no. 9, pp. 1958–1975, Sep. 2009.
- [22] S. Baker and T. Kanade, "Limits on super-resolution and how to break them," *IEEE Trans. Pattern Anal. Mach. Intell.*, vol. 24, no. 9, pp. 1167–1183, Sep. 2002.
- [23] W. T. Freeman, T. R. Jones, and E. C. Pasztor, "Example-based superresolution," *IEEE Comput. Graph. Appl.*, vol. 22, no. 2, pp. 56–65, Mar./Apr. 2002.
- [24] H. Chang, D.-Y. Yeung, and Y. Xiong, "Super-resolution through neighbor embedding," in *Proc. IEEE Conf. Comput. Vis. Pattern Recog.*, Jul. 2004, pp. 275–282.
- [25] S. T. Roweis and L. K. Saul, "Nonlinear dimensionality reduction by locally linear embedding," *Science*, vol. 290, no. 5500, pp. 2323–2326, Dec. 2000.
- [26] T.-M. Chan and J. Zhang, "An improved super-resolution with manifold learning and histogram matching," in *Proc. IAPR Int. Conf. Biometric*, 2006, pp. 756–762.
- [27] T.-M. Chan, J. Zhang, J. Pu, and H. Huang, "Neighbor embedding based super-resolution algorithm through edge detection and feature selection," *Pattern Recognit. Lett.*, vol. 30, no. 5, pp. 494–502, Apr. 2009.
- [28] W. Fan and D. Y. Yeung, "Image hallucination using neighbor embedding over visual primitive manifolds," in *Proc. IEEE Conf. Comput. Vis. Pattern Recog.*, Jun. 2007, pp. 1–7. 480 *IEEE TRANSACTIONS ON IMAGE PROCESSING*, VOL. 21, NO. 2, FEBRUARY 2012.
- [29] B. Li, H. Chang, S. Shan, and X. Chen, "Locality preserving constraints for super resolution with neighbor embedding," in *Proc. IEEE Int. Conf. Image Process.*, Nov. 2009, pp. 1189–1192.
- [30] K. Zhang, X. Gao, X. Li, and D. Tao, "Partially supervised neighbour embedding for example-based image super-resolution," *IEEE J. Sel. Topics Signal Process.*, vol. 5, no. 2, pp. 230–239, Apr. 2011.
- [31] T. Zhou, D. Tao, and X. Wu, "Manifold elastic net: A unified framework for sparse dimension reduction," *Data Mining Knowl. Discov.*, vol. 22, no. 3, pp. 340–371, May 2011.
- [32] D. Tao, X. Li, X. Wu, and S. J. Maybank, "Geometric mean for subspace selection," *IEEE Trans. Pattern Anal. Mach. Intell.*, vol. 31, no. 2, pp. 260–274, Feb. 2009.
- [33] W. Bian and D. Tao, "Biased discriminant Euclidean embedding for content based image retrieval," *IEEE Trans. Image Process.*, vol. 19, no. 2, pp. 545–554, Feb. 2010.
- [34] J. Yang, J. Wright, T. Huang, and Y. Ma, "Image super-resolution as sparse representation of raw image patches," in *Proc. IEEE Conf. Comput. Vis. Pattern Recog.*, Jun. 2008, pp. 1–8.
- [35] J. Yang, J. Wright, T. Huang, and Y. Ma, "Image super-resolution via sparse representation," *IEEE Trans. Image Process.*, vol. 19, no. 11, pp. 2861–2873, Nov. 2010.
- [36] M. Song, D. Tao, C. Chen, X. Li, and C. W. Chen, "Color to gray: Visual cue preservation," *IEEE Trans. Pattern Anal. Mach. Intell.*, vol. 32, no. 9, pp. 1537–1552, Sep. 2010.
- [37] K. Su, Q. Tian, Q. Que, N. Sebe, and J. Ma, "Neighborhood issue in single-frame image super-resolution," in *Proc. IEEE Int. Conf. Multimedia Expo*, Jul. 2005, pp. 1122–1125.
- [38] W. Bian and D. Tao, "Max-min distance analysis by using sequential SDP relaxation for dimension reduction," *IEEE Trans. Pattern Anal. Mach. Intell.*, vol. 33, no. 5, pp. 1037–1050, May 2011.
- [39] S. Si, D. Tao, and B. Geng, "Bregman divergence based regularization for transfer subspace learning," *IEEE Trans. Knowl. Data Eng.*, vol. 22, no. 7, pp. 929–942, Jul. 2010.
- [40] D. Tao, X. Li, X. Wu, and S. J. Maybank, "General tensor discriminant analysis and gabor features for gait recognition," *IEEE Trans. Pattern Anal. Mach. Intell.*, vol. 29, no. 10, pp. 1700–1715, Oct. 2007.
- [41] M. Irani and S. Peleg, "Motion analysis for image enhancement: Resolution, occlusion and transparency," *J. Vis. Commun. Image Represent.*, vol. 4, no. 4, pp. 324–335, Dec. 1993.
- [42] Xinbo Gao, Kaibing Zhang, Dacheng Tao, and Xuelong Li, "Combine Learning for Single-Image Super-Resolution via a Coupled Constraint," *IEEE Trans. Image Process.*, Vol. 21, no. 2, February 2012.
- [43] Y. Tang, P. Yan, Y. Yuan, and X. Li, "Single-image super resolution via local learning," *Int. J. Mach. Learn. Cybern.*, vol. 2, no. 1, pp. 15–23, Mar. 2011, DOI: 10.1007/s13042-011-0011-6.